J. Amer. Soc. Hort. Sci. 147(5):249–259. 2022. https://doi.org/10.21273/JASHS05222-22

Identification and Functional Analysis of MicroRNAs and Their Target Genes in Reverse Thermosensitive Genic Male Sterility of Eggplant

Bing Li, Jingjing Zhang, Xiurui Gao, and Xiuqing Pan
Institute of Cash Crops, Hebei Academy of Agriculture and Forestry Sciences, Shijiazhuang, 050051, China

Rong Zhou
Department of Food Science, Aarhus University, Aarhus N, DK-8200, Denmark

Yanrong Wu
Institute of Cash Crops, Hebei Academy of Agriculture and Forestry Sciences, No. 598 Heping West Road, Shijiazhuang, 050051, China

Additional index words. anther development, low temperature, miRNA, regulatory network, small RNA sequencing, *Solanum melongena*

Abstract. **Thermosensitive genic male sterile (TGMS) lines are the core of two-line hybrid systems. MicroRNAs (miRNAs) play critical roles in plant growth and development. However, knowledge of regulation of anther development by miRNAs in TGMS eggplant (*Solanum melongena*) is largely unexplored. To investigate the mechanism underlying miRNA regulation of male sterility, we employed high-throughput small RNA sequencing in anther samples from the reverse TGMS line 05ms and the temperature-insensitive line S63 in eggplant, under high temperature and low temperature conditions. The 05ms line is sterile at low temperature and fertile at high temperature. A total of 166,273,427 raw reads were obtained, 143 known miRNAs from 42 miRNA families and 104 novel miRNAs were detected. Further, six differentially expressed miRNAs (DEMs) were identified, including three known (miR168b-3p, miR397–5p, and miR408) and three novel miRNAs (Novel_116, Novel_119, and Novel_97), which might be related to anther development. Moreover, the six DEMs were validated by quantitative real-time polymerase chain reaction and 892 target genes of which were predicted. Gene Ontology analysis of target genes revealed significant enrichment in the "copper ion binding," "oxidation-reduction process," and "oxidoreductase activity" terms. Kyoto Encyclopedia of Genes and Genomes analysis revealed that "plant hormone signal transduction" and "other glycan degradation" were enriched. In addition, we constructed regulatory networks comprising miRNAs, target genes, and important terms/pathways and found the miR397-5p was the most linked miRNA, down-regulated under low temperature. Our findings contribute to understanding of the roles of miRNA during anther development and provide the theoretical foundation for two-line hybrid breeding of eggplant.**

Eggplant (*Solanum melongena*) is an important vegetable globally. With rising labor costs, it is estimated that the utilization of eggplant with male sterility will play a greater role in their cultivation. Hybrid seed production using male sterile lines mainly involves the three- and two-line hybrid systems. The three-line hybrid system requires male sterile, restorer, and maintainer lines, whereas the two-line system involves an environmentally sensitive genic male sterile (EGMS) line, such as a photoperiod-sensitive or thermosensitive genic male sterile (PGMS or TGMS) line, which is used to produce hybrid seeds, thus eliminating the need for maintainer and restorer lines (Sun et al., 2021). Hence, the two-line system is more convenient for hybrid seed production (Zhou et al., 2016). The EGMS lines have been reported in some vegetable crops, including tomato [*Solanum lycopersicum* (Sheoran et al., 2009)] and eggplant (Li et al., 2019).

miRNAs are a class of small endogenous non-coding RNAs. Since the first report of miRNAs in rabidopsis [*Arabidopsis thaliana* (Llave et al., 2002)], there has been considerable research aimed at understanding their molecule mechanism (Voinnet, 2009). The miRNAs comprise ≈21 to 24 nucleotides and function as negative regulators of gene expression by degrading mRNA or inhibiting translation (Betti et al., 2021). Extensive research has demonstrated critical roles for miRNAs in regulation of various biological processes (Feng et al., 2019; Shi et al., 2019), including organ development and hormone signaling, as well as responses to abiotic stresses (Lin et al., 2020). Plants are more vulnerable to environmental stresses, such as low temperature or high temperature at the reproductive growth stage than during the vegetative growth phase (Tang et al., 2012). Numerous studies have identified the roles of miRNAs in regulating plant male sterility primarily by inhibiting target genes that affect anther development (Dong et al., 2020) and regulate fertility (Jiang et al., 2021). The male sterility in eggplant was induced by suppressing TATA box-binding protein associated factors using artificial miRNA technology (Toppino et al., 2011). Thirteen

Received for publication 18 Apr. 2022. Accepted for publication 1 July 2022. Published online 12 August 2022.
This research was funded by the Scientific and Technological Innovation Talent Team Construction Project of Hebei Academy of Agriculture and Forestry Sciences (grant no. C21R0802), the Basic Scientific Research Fund of Hebei Academy of Agriculture and Forestry Sciences (grant no. 2021050202), the National Bulk Vegetable Industry Technology System Project (grant no. CARS-23-G-05), and the Third Round of the "Giant Plan" Vegetable Scientific Research and Innovation Team project in Hebei Province.
Y.W. is the corresponding author. E-mail: jzswuyanrong@163.com.
This is an open access article distributed under the CC BY-NC-ND license (https://creativecommons.org/licenses/by-nc-nd/4.0/).

Downloaded from https://prime-pdf-watermark.prime-prod.pubfactory.com/ at 2025-07-30 via Open Access. This is an open access article distributed under the CC BY-NC-ND license (https://creativecommons.org/licenses/by-nc-nd/4.0/). https://creativecommons.org/licenses/by-nc-nd/4.0/

pairs of miRNA/target genes that regulate male sterility in PGMS/TGMS rice (*Oryza sativa*) by responding to temperature change were identified by miRNA, transcriptome, and degradome sequencing, and miR156, miR5488, and miR399 were found to affect male sterility in PA64S by influencing anther wall lignin synthesis and the flavonoid metabolism pathway (Sun et al., 2021).

Reactive oxygen species (ROS) and phytohormones are two important signaling systems involved in plant responses to abiotic stress, and drive changes that guide plant adaptation and survival (Devireddy et al., 2021). Cellular reduction/oxidation (redox) homeostasis plays an important role in balancing temperature tolerance and plant development (Concetta et al., 2015). High temperature during the anthesis stage causes a significant rise in ROS content accumulation in anthers, triggering male sterility due to differential antioxidant enzyme activity-mediated anther damage (Dwivedi et al., 2019). Phytohormones also play essential roles during anther development processes (Zhang et al., 2021). Research into a wheat (*Triticum aestivum*) TGMS line indicated that six miRNAs and one transacting small interfering RNA regulated the auxin signaling network, which are linked with male sterility during cold stress (Tang et al., 2012). Further, arabidopsis transgenic phenotypes of *auxin response factor 6* (*arf6*) plants mutated miR167 target sites suggest that miR167 may repress *ARF6* translation, preventing proper pollen release from anthers (Zheng et al., 2019). Abscisic acid (ABA) is a key phytohormone that regulates plant development and responses to biotic and abiotic stresses (Yoshida et al., 2015). *MYB33* is a major target of miR159, which promotes *ABA Insensitive 5* (*ABI5*) transcription through directly binding to its promoter. The *ABI5* promotes vegetative phase development in arabidopsis by affecting expression of the miR156-SPL pathway (Guo et al., 2021). *MYB33* and *SPL* were genes that regulate early development of tapetum in rice (Huang et al., 2011). miR397a was up-regulated in ABA-deficient mutant rice (Tian et al., 2015). Moreover, miRNAs and their target genes have vital functions in male fertility, lignin formation, and adaptation to abiotic stress in rice (Tian et al., 2015). miR408 and miR397 were both negatively regulated by copper, an essential mineral required for plant development, and their target genes encoded copper-containing proteins, including *laccase* (*LAC*) in arabidopsis (Abdel-Ghany and Pilon, 2008).

Eggplant is a thermophilic plant; hence, low temperature is an important abiotic stress that influences its growth and development (Yang et al., 2017). The reverse TGMS (rTGMS) eggplant line 05ms is sterile at low temperature and fertile at high temperature (Li et al., 2019). Abundant evidence supports key roles for miRNAs in the regulation of anther development in many crops. However, there have been no reports regarding miRNA expression in eggplant anther. To address this, we performed small RNA sequencing (sRNA-seq) of samples from anthers (meiosis stage) of the 05ms and S63 eggplant lines cultivated under low temperature and high temperature. Two coexpression networks, comprising Gene Ontology (GO) terms, Kyoto Encyclopedia of Genes and Genomes (KEGG) pathways, miRNAs, and target genes, were constructed, and genes with pivotal roles were discovered. Further, a candidate miRNA with a role in regulating rTGMS was predicted, and a mechanism by which it can potentially result in temperature-dependent fertility conversion was discovered. Our data provide a valuable information for miRNA research in eggplant for hybridization breeding, which broaden our understanding of the mechanisms underlying fertility conversion in rTGMS lines in plants.

Materials and Methods

Plant materials, cultivation environment, and tissue collection. Two inbred eggplant lines, rTGMS line 05ms and the fertile line S63, were used as the experimental materials (Supplemental Fig. 1). The rTGMS line was a natural mutation from S63. Plant seeds were sown on 3 Jan. 2020 in a greenhouse in Shijiazhuang (lat. 38.03°N, long. 114.26°E), Hebei province, China. When the plants grew to five to six true leaves (15 Apr.), seedlings of each line were planted in plastic greenhouse, where a self-measuring thermometer was placed. The rTGMS line 05ms exhibits male sterility at $<18.0\,^{\circ}C$ and is fully fertile at $>19.5\,^{\circ}C$. Anthers samples at meiosis stage were collected at the sterile period of spring low temperature from 05ms (05ms-spring), the fertile period of summer high temperature from 05ms (05ms-summer), and the fertile period of spring low temperature from S63 (S63-spring), the fertile period of summer high temperature from S63 (S63-summer). Samples were taken in late April and early June. Each time, ≈10 to 15 flower buds were taken from five plants as a sample, and quickly peeled off the ovary and petals, collected the anthers, placed them in a 1.5-mL centrifuge tube, and rapidly transferred into liquid nitrogen (–196 °C). There were 12 samples in total (05ms-spring, 05ms-summer, S63-spring, and S63-summer, three biological replicates). Samples were taken back to the laboratory and stored in an ultra-low temperature freezer (–80 °C) for RNA extraction.

RNA extraction and detection. Total RNA was extracted from anther by using the DP441 RNA extraction Kit (Tiangen Biotech Co., Ltd., Beijing, China) according to the manufacturer's instructions. RNA degradation and contamination was monitored on 1% agarose gels. RNA purity was checked using a spectrophotometer (NanoPhotometer; IMPLEN, Westlake Village, CA). RNA concentration was measured using RNA Assay Kit in a flurometer (Qubit 2.0; Life Technologies, Carlsbad, CA). RNA integrity was assessed using the RNA Nano 6000 Assay Kit of an automated electrophoresis tool (Bioanalyzer 2100; Agilent Technologies, Palo Alto, CA).

sRNA library construction and sequencing. Twelve samples from four treatments (05ms-spring, 05ms-summer, S63-spring, and S63-summer, three biological replicates) were sent to Novogene Bioinformatics Technology Co. Ltd. (Beijing, China) for sRNA-seq analysis. A total amount of 3 μg RNA per sample was used as input material for the sRNA library. Sequencing libraries were generated using NEBNext Multiplex sRNA Library Prep Set for Illumina (NEB, Ipswich, MA) following the manufacturer's recommendations, and index codes were added to attribute sequences to each sample. Polymerase chain reaction (PCR) products were purified on a 8% polyacrylamide gel (100 V, 80 min). DNA fragments corresponding to 140 to 160 bp (the length of small noncoding RNA plus the 3' and 5' adaptors) were recovered and dissolved in 8-μL elution buffer. Library quality was then assessed on the automated electrophoresis tool (Bioanalyzer 2100) using DNA High Sensitivity Chips (Agilent Technologies, Santa Clara, CA). The clustering of the index-coded samples was performed on a cBot Cluster Generation System using TruSeq SR Cluster Kit v3-cBot-HS (Illumia, San Diego, CA) according to the manufacturer's instructions. After cluster generation, the library preparations

Downloaded from https://prime-pdf-watermark.prime-prod.pubfactory.com/ at 2025-07-30 via Open Access. This is an open access article distributed under the CC BY-NC-ND license (https://creativecommons.org/licenses/by-nc-nd/4.0/). https://creativecommons.org/licenses/by-nc-nd/4.0/

were sequenced on an Illumina HisEq. 2500 platform and 50 bp single-end reads were generated. The raw data were deposited into the National Center for Biotechnology Information Sequence Read Archive with accession number PRJNA791470.

sRNA-seq data analysis. Clean data (clean reads) were obtained by removing reads using Cutadapt software. The sequence quality was verified using FastQC (Wingett and Andrews, 2018). Then, unique sequences (18 to 30 nt long) were chosen from clean reads to do all the downstream analyses. To prevent every unique sRNA mapping to multiple noncoding RNA, we used the following priority rule: known miRNA > ribosomal RNA (rRNA) > transfer RNA (tRNA) > small nuclear RNA (snRNA) > small nucleolar RNA (snoRNA) > repeat > gene > novel miRNA; this ensured that every unique sRNA mapped to only one annotation. sRNA tags were mapped to reference sequences (Hirakawa et al., 2014) using bowtie-0.12.9 (Langmead et al., 2009). The known and novel miRNAs and secondary structures drawn were identified by BLAST search with the miRBase22.1 database, modified software mirdeep2 (Friedlander et al., 2011), and sRNA-tools-cli. To remove tags originating from protein-coding genes, repeat sequences, rRNA, tRNA, snRNA, and snoRNA, sRNA tags were mapped to RepeatMasker, Rfam database, or those types of data from the specified species itself. In our analysis pipeline, families of known miRNAs were determined using miFam.dat (Kozomara et al., 2019), and novel miRNA precursors were submitted to Rfam (Nawrocki et al., 2015) to search for Rfam families. miRNA expression levels were estimated as transcripts per million, using previously described criteria (Zhou et al., 2010).

Identification of differentially expressed miRNA and target gene. Analysis of differential expression between two groups was performed using the DESeq2 package ver. 3.0.3 (Love et al., 2014). The following criteria were used to identify significantly upregulated and downregulated miRNAs: $|\log2(\text{fold change})| > 1$ and adjusted $P < 0.05$. miRNA target genes were predicted using psRobot_tar in psRobot for plants (Wu et al., 2012).

GO and KEGG enrichment analysis of target gene. GO enrichment analysis was used on the target gene candidates of differentially expressed miRNAs (DEMs) in the following. GOseq based Wallenius noncentral hypergeometric distribution (Young et al., 2010), which could adjust for gene length bias, was implemented for GO enrichment analysis. KEGG is a database resource for understanding high-level functions and utilities of the biological system, such as the cell, the organism and the ecosystem, from molecular-level information, especially large-scale molecular datasets generated by genome sequencing and other high-throughput experimental technologies (Kanehisa et al., 2008). We used KOBAS (Mao et al., 2005) software to test the statistical enrichment of the target gene candidates in KEGG pathways.

Quantitative real-time PCR analysis. Total miRNA samples were extracted from frozen anthers using a DP501 kit (Tiangen Biotech Co., Ltd.). miRNA First-Strand cDNA was synthesized using a KR201 Kit (Tiangen Biotech Co., Ltd.). An miRcute miRNA Detection Kit (FP401; Tiangen Biotech Co., Ltd.) was then used to quantify known miRNAs following the manufacturer's instructions. Six DEMs were analyzed by quantitative real-time (qRT)-PCR with U6 as a reference. The miRNA forward primers are listed in Supplemental Table 1, and the reverse primer was a universal primer provided in the FP401 kit. Assays were performed on a CFX ConnectTM instrument (Bio-Rad Laboratories, Hercules, CA) using the following program: 94 °C for 2 min, followed by 40 cycles at 94 °C for 20 s and 60 °C for 30 s. Target genes of miRNAs were analyzed by qRT-PCR following a previously published method (Li et al., 2019). The primers are listed in Supplemental Table S, and actin was used as a reference. Data were analyzed using the $2^{-\text{ppCT}}$ method (Schmittgen and Livak, 2008).

Analysis of concentrations of physiological and biochemical indices. ABA concentrations were detected on the testing platform (QTRAP 6500 LC-MS/MS; AB Sciex, Framingham, MA). Hydrogen peroxide and catalase (CAT) concentrations were measured using the H_2O_2-1-Y and CAT-1-Y kits (Comin Biotechnology Co., Ltd., Suzhou, China) with a testing tool (Cytation 1; BioTek Instruments Inc., Winooski, VT). Statistical analysis software (IBM SPSS Statistics ver. 18.0; IBM Corp., Armonk, NY) was used to conduct analysis of variance and the *t* test to compare 05ms-summer to 05ms-spring for each category. $P < 0.05$ was considered statistically significant in all analyses. Figures were prepared with an analysis software (Prism 8.0.2; GraphPad Software Inc., San Diego, CA). All data were averaged over three biological replicates.

Results

Overview of sRNA library sequencing data. To investigate the roles of miRNAs in response to temperature variation during anther development in 05ms, 12 sRNA libraries (three biological replicates respectively for 05ms-spring, 05ms-summer, S63-spring, and S63-summer) were constructed and a total of 166,273,427 raw data were obtained using the Illumina sequencing platform. After removing low-quality reads, 39,602,285 (05ms-spring), 41,921,223 (05ms-summer), 40,774,449 (S63-spring), and 39,515,432 (CH) clean reads were obtained, respectively (Supplemental Table 2). More than 90% of these sRNA could be mapped to reference sequences (Supplemental Table 3). sRNAs in all sequencing libraries were categorized. Interestingly, there were fewer rRNA, snRNA, and snoRNA in the 05ms line than in the S63 line in anthers from plants grown under both high and low temperature conditions (Table 1). sRNAs within specific length ranges were then selected for the subsequent analysis of sRNA distribution. The 18–30 nt sRNAs were dominant in all libraries. Among these, the most abundant sRNAs were 24 nt siRNAs (>40%), followed by 21–22 nt miRNA (10% to 15%; Fig. 1A). We analyzed the first nucleotide bias and found 20–23 nt miRNAs mostly starting with "U" as the first base, with "C" the first base in most 21 nt molecules from the 05ms-spring group. Further, 24-nt miRNAs mostly started with an 'A' residue in the S63-summer and 05ms-spring groups, whereas they began with "U" in the 05ms-summer and S63-spring groups (Fig. 1B). Next, sRNAs screened for length were matched to reference genome. A total of 143 known miRNAs and 104 novel miRNAs were detected in anthers from the four groups. These miRNAs belonged to 42 miRNA families by comparing them in Solanaceae crops, with miR156, miR166, miR395, miR169_2, miR172, and miR399 as the top six families (Fig. 1C).

Identification of rTGMS-related miRNAs and their target genes. To identify miRNAs related to anther development and fertility conversion in eggplant, we screened for

Downloaded from https://prime-pdf-watermark.prime-prod.pubfactory.com/ at 2025-07-30 via Open Access. This is an open access article distributed under the CC BY-NC-ND license (https://creativecommons.org/licenses/by-nc-nd/4.0/). https://creativecommons.org/licenses/by-nc-nd/4.0/

Table 1. Categorization of unique reads and total reads of small RNA (sRNA) in the sterile line 05ms and fertile line S63 of eggplant.

	S63-summer[ii]		S63-spring		05ms-summer		05ms-spring	
Type[i]	n	%	n	%	n	%	n	%
Total sRNA	21,351,798	100.00	31,377,617	100.00	34,489,484	100.00	29,492,934	100.00
Known_miRNA	293,499	1.37	740,515	2.36	277,559	0.80	199,006	0.67
rRNA	2,958,339	13.86	7,045,340	22.45	3,443,386	9.98	2,832,789	9.60
tRNA	979,408	4.59	322,429	1.03	594,220	1.72	560,505	1.90
snRNA	11,873	0.06	31,077	0.10	12,801	0.04	12,290	0.04
snoRNA	69,039	0.32	274,223	0.87	59,478	0.17	76,749	0.26
Repeat	1,531,812	7.17	2,095,096	6.68	2,658,883	7.71	2,228,272	7.56
Novel_miRNA	222,819	1.04	149,822	0.48	197,517	0.57	115,336	0.39
Other	9,713,590	45.49	12,385,040	39.47	17,331,652	50.25	14,909,604	50.55

[i] miRNA = micro RNA; rRNA = ribosomal RNA; tRNA = transfer RNA; snRNA = small nuclear RNA; snoRNA = small nucleolar RNA.
[ii] S63-summer = summer fertile period at high temperature in S63; S63-spring = spring fertile period at low temperature in S63; 05ms-summer = summer fertile period at high temperature in 05ms; 05ms-spring = spring sterile period at low temperature in 05ms.

DEMs in the 05ms-spring, 05ms-summer, S63-spring, and S63-summer libraries. DEMs were identified based on threshold values: false discovery rate < 0.05 and |log2 (fold-change)| > 1. Most DEMs (n = 113) were identified in the 05ms-spring vs. S63-spring groups, among which 61 and 52 miRNAs were upregulated and downregulated in 05ms-spring, respectively. Only 41 DEMs were identified in comparisons of both 05ms-spring vs. 05ms-summer and 05ms-summer vs. S63-summer (Fig. 2A).

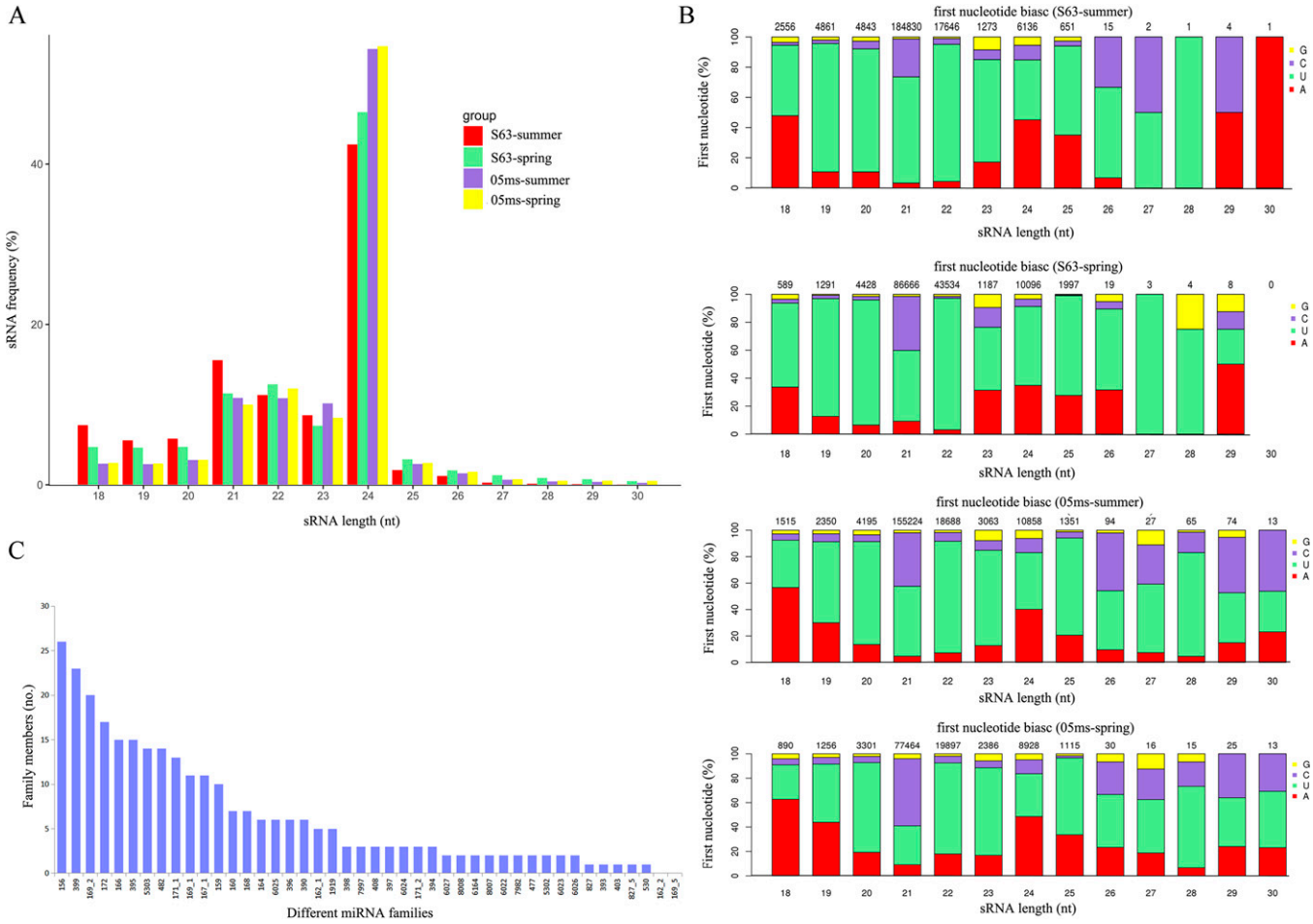

Fig. 1. The character analysis of small RNA (sRNA) in the sterile line 05ms and fertile line S63 of eggplant. (**A**) The length distribution of sRNAs. (**B**) The first nucleotide bias analysis of known sRNAs. (**C**) The microRNA (miRNA) families analysis of known miRNAs (05ms-spring = spring sterile period at low temperature in 05ms; 05ms-summer = summer fertile period at high temperature in 05ms; S63-spring = spring fertile period at low temperature in S63; S63-summer = summer fertile period at high temperature in S63). sRNA frequency represents the percentage of sRNA among S63-summer, S63-spring, 05ms-summer, and 05ms-spring under different length. First nucleotide represents the percentage of A/U/C/G in the first base of sRNA of this length. The numbers above each bar represent the total numbers of sRNA of this length. Different miRNA families were detected in the Solanaceae crops. Family numbers represent the numbers of different miRNA families.

Downloaded from https://prime-pdf-watermark.prime-prod.pubfactory.com/ at 2025-07-30 via Open Access. This is an open access article distributed under the CC BY-NC-ND license (https://creativecommons.org/licenses/by-nc-nd/4.0/). https://creativecommons.org/licenses/by-nc-nd/4.0/

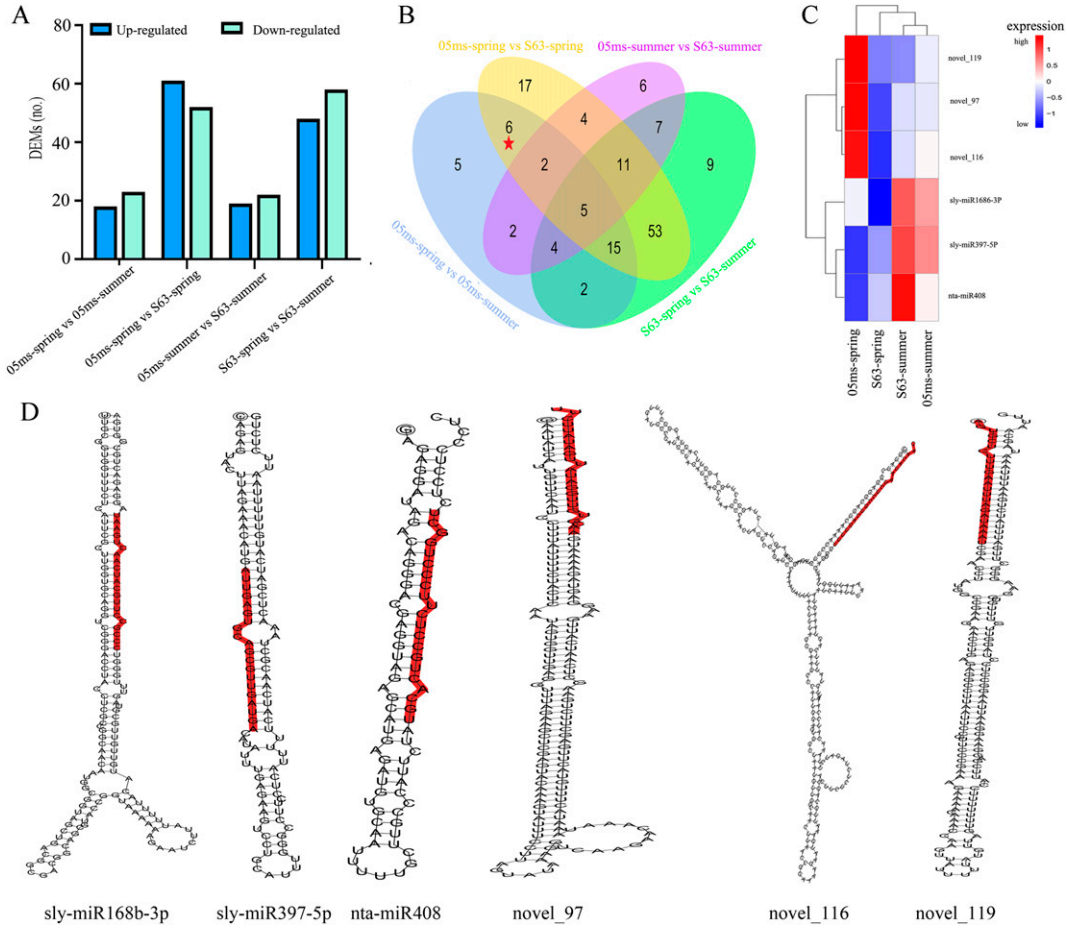

Fig. 2. Analysis of differential expression levels and secondary structures of microRNAs (miRNAs) in the sterile line 05ms and fertile line S63 of eggplant. (**A**) Numbers of differentially expressed miRNAs (DEMs) in different comparisons. (**B**) Venn diagram showing the overlaps in different comparisons. (**C**) Heatmap showing the hierarchical cluster analysis results from samples and DEMs. (**D**) Secondary structures of DEMs. DEMs represents the numbers of DEMs. "Upregulated" indicates upregulated DEMs. Downregulated indicates downregulated DEMs (05ms-spring = spring sterile period at low temperature in 05ms; 05ms-summer = summer fertile period at high temperature in 05ms; S63-spring = spring fertile period at low temperature in S63; S63-summer = summer fertile period at high temperature in S63). The red star indicates the key DEMs. Each column indicates sample, and the colored bar indicates the relative expression level from high (red) to low (blue). Red highlights indicate the locations of mature sequence of miRNA.

These findings suggest that some miRNAs were only expressed in the sterile line during the 05ms-spring period.

Venn diagram analysis of DEMs showed that six DEMs were most closely related to sterility because they did not differ significantly when comparing anther fertility groups (05ms-summer vs. S63-summer and S63-spring vs. S63-summer), but there were significant differences when comparing anther sterility groups (05ms-spring vs. S63-spring and 05ms-spring vs. 05ms-summer; Fig. 2B). Among these six DEMs, three novel miRNAs (Novel_116, Novel_119, and Novel_97) were upregulated in 05ms-spring, with Novel_97 the most significantly altered. The other three DEMs (nta-miR408, sly-miR168b-3p, and sly-miR397–5p), downregulated in 05ms-spring, were known miRNAs, with sly-miR397-5p the most significantly difference (Fig. 2C, Supplemental Table 4). The secondary structures of the six miRNAs are shown in Fig. 2D.

We performed qRT-PCR to verify further the expression of the six DEMs between 05ms and S63. The results of qRT-PCR were consistent with those of sRNA-seq (Fig. 3, Supplemental Table 5). Software analysis predicted 892 target genes for the six identified miRNAs. The target genes of miR397–5p were predicted, and 382 target genes were found, including transcription factors *dysfunctional tapetum 1* (*dyt1*) and *WRKY*, and many *LAC* family genes. We verified the expression levels of four target genes by qRT-PCR and found the expression levels were opposite of miR397-5p in 05ms, thus further confirming that they were underlying target genes of miR397-5 (Supplemental Fig. 2). The four target genes of miR397–5p were *Sme2.5_00016.1_g00020.1* (*WRKY32*), *Sme2.5_05438.1_g00004.1* (*dyt1*), *Sme2.5_01800.1_g00006.1* (*LAC4*), and *Sme2.5_02906.1_g00004.1* (*LAC4*).

Biological function analysis of target genes. The regulatory function of miRNA is executed through its target genes. To further understand the biological functions of miRNAs, annotations of the 892 target genes were classified into three GO categories: molecular function (29.86%), biological process (55.43%), and cellular component (14.71%) (Fig. 4A). Significant terms included "copper ion binding" [GO: 0005507 (n = 21)], "oxidation-reduction process" [GO: 0055114 (n = 59)], and "oxidoreductase activity" [GO: 0016491 (n = 60)]. These results suggest that the redox is an important factor in rTGMS fertility conversion. The detailed information of the first 20 terms in GO functional enrichment analysis are listed in Supplemental Table S6.

To further explore our findings, KEGG enrichment analysis of 892 target genes was conducted. The target genes were

Downloaded from https://prime-pdf-watermark.prime-prod.pubfactory.com/ at 2025-07-30 via Open Access. This is an open access article distributed under the CC BY-NC-ND license (https://creativecommons.org/licenses/by-nc-nd/4.0/). https://creativecommons.org/licenses/by-nc-nd/4.0/

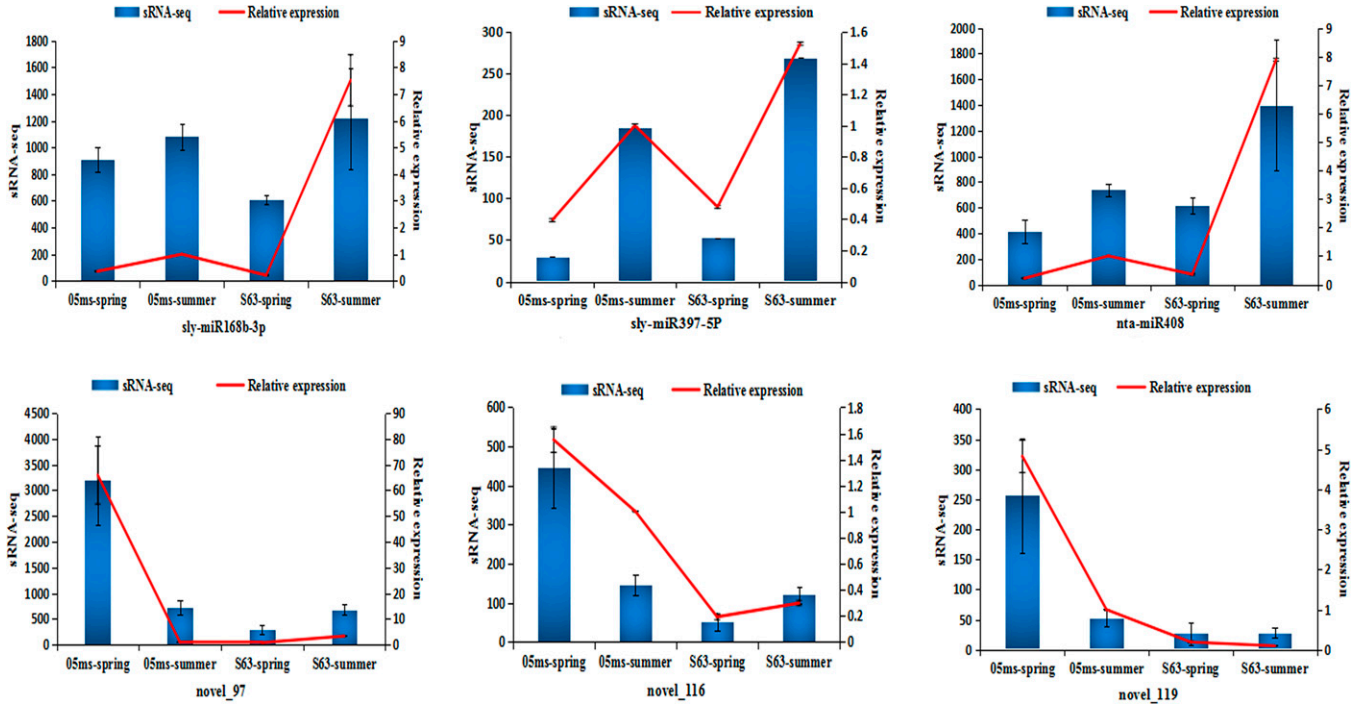

Fig. 3. Comparison of results obtained via small RNA sequencing (sRNA-seq) and quantitative real-time PCR (qRT-PCR) for the six differentially expressed microRNAs (DEMs) at different periods in the sterile line 05ms and fertile line S63 of eggplant. miR168b-3p, miR397–5p, and miR408, Novel_116, Novel_119, and Novel_97 were the six DEMs (05ms-spring = spring sterile period at low temperature in 05ms; 05ms-summer = summer fertile period at high temperature in 05ms; S63-spring = spring fertile period at low temperature in S63; S63-summer = summer fertile period at high temperature in S63). Error bars indicate the SE of three biological replicates.

mapped to 72 biological pathways, and the top 20 pathways of KEGG functional enrichment analysis is shown in Fig. 4B. Most target genes were enriched in "plant hormone signal transduction" [sly04075 (n = 7)], "biosynthesis of amino acids" [sly01230 (n = 6)], and "spliceosome" [sly03040 (n = 6)]. The pathways "other glycan degradation" [sly00511 (n = 3)],

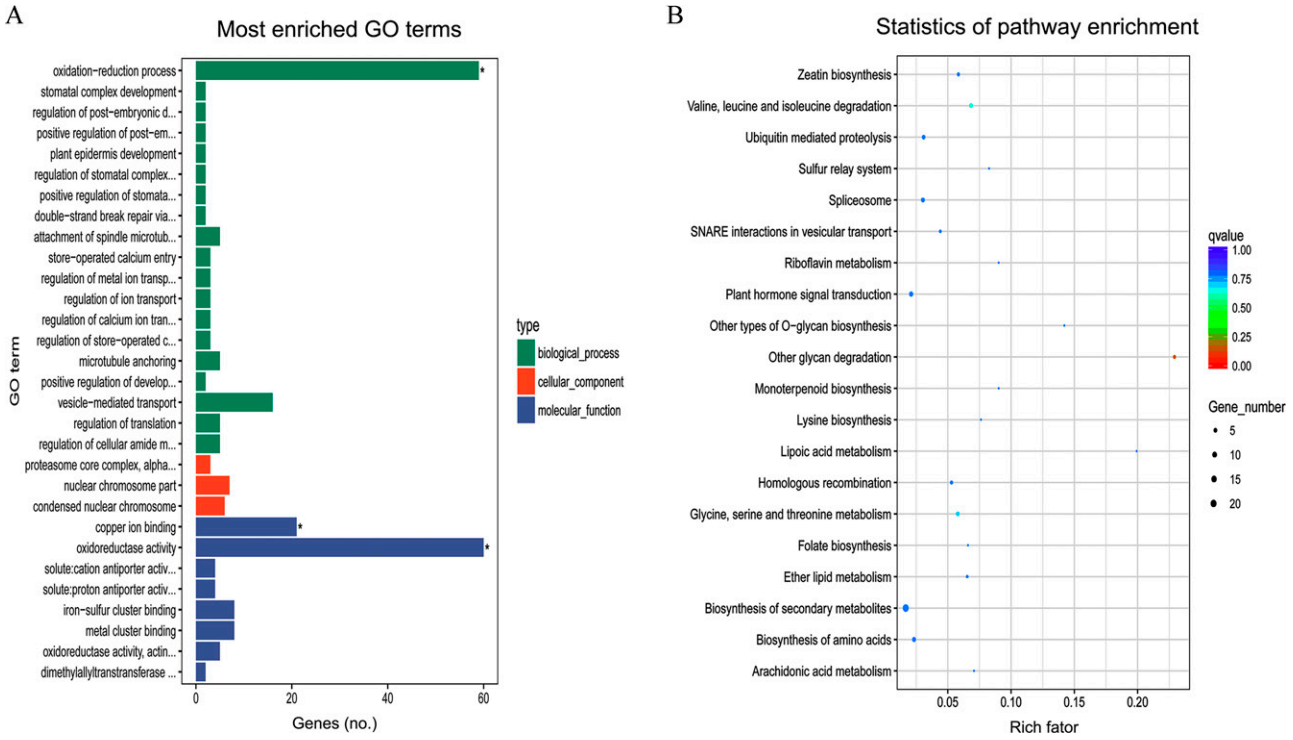

Fig. 4. Gene Ontology (GO) terms and Kyoto Encyclopedia of Genes and Genomes (KEGG) pathways enrichment analysis of the 892 target genes in the sterile line 05ms and fertile line S63 of eggplant. (**A**) The top 20 significantly enriched GO terms. (**B**) The top 20 significantly enriched KEGG pathways.

Downloaded from https://prime-pdf-watermark.prime-prod.pubfactory.com/ at 2025-07-30 via Open Access. This is an open access article distributed under the CC BY-NC-ND license (https://creativecommons.org/licenses/by-nc-nd/4.0/). https://creativecommons.org/licenses/by-nc-nd/4.0/

"valine, leucine and isoleucine degradation" [sly00280 (n = 4)], and "glycine, serine and threonine metabolism" [sly00260 (n = 3)] were also particularly noteworthy. The detailed information of the 72 terms in KEGG functional enrichment analysis is listed in Supplemental Table 7.

miRNA-mRNA regulatory network analysis. To functionally characterize DEMs and their target genes, we built regulatory networks including significant GO terms and KEGG pathways. The three GO terms included in the regulatory network comprised 64 target genes and five miRNAs (Fig. 5). Further, three KEGG pathways in the regulatory network included 11 target genes and 4 miRNAs (Fig. 6). Five genes were targeted by sly-miR397-5p, three of which (*Sme2.5_31020.1_g00001.1*, *Sme2.5_09769.1_g00002.1*, and *Sme2.5_00110.1_g00020.1*) were redox (dehydrogenase) enzymes. The sly-miR397-5p was the most linked in both the KEGG and GO networks, which could be a key miRNA in eggplant thermosensitive male sterility.

ABA, H_2O_2, and CAT content in 05ms anthers. According to our previous research results, ABA and ROS had significant influence on male sterility of eggplant. Thus, ABA, H_2O_2, and CAT content in '05ms' anthers from the 05ms-spring and 05ms-summer were detected. ABA and H_2O_2 were higher and CAT was lower in 05ms-spring than in 05ms-summer (Fig. 7). The content of ABA was 41.50 U/g in 05ms-spring, which was 2.16-fold higher than that in 05ms-summer. H_2O_2 content was 1.70-fold higher in 05ms-spring (2.52 $\mu mol \cdot g^{-1}$) than in 05ms-summer. In particular, the largest difference was that in CAT content, which was 4.02-fold higher in 05ms-summer (3184.18 $nmol \cdot g^{-1} \cdot min^{-1}$) than in 05ms-spring (792.48 $nmol \cdot g^{-1} \cdot min^{-1}$).

Discussion

Heterosis is a useful way to increase yield and improve eggplant quality. TGMS lines represent excellent germplasm resources

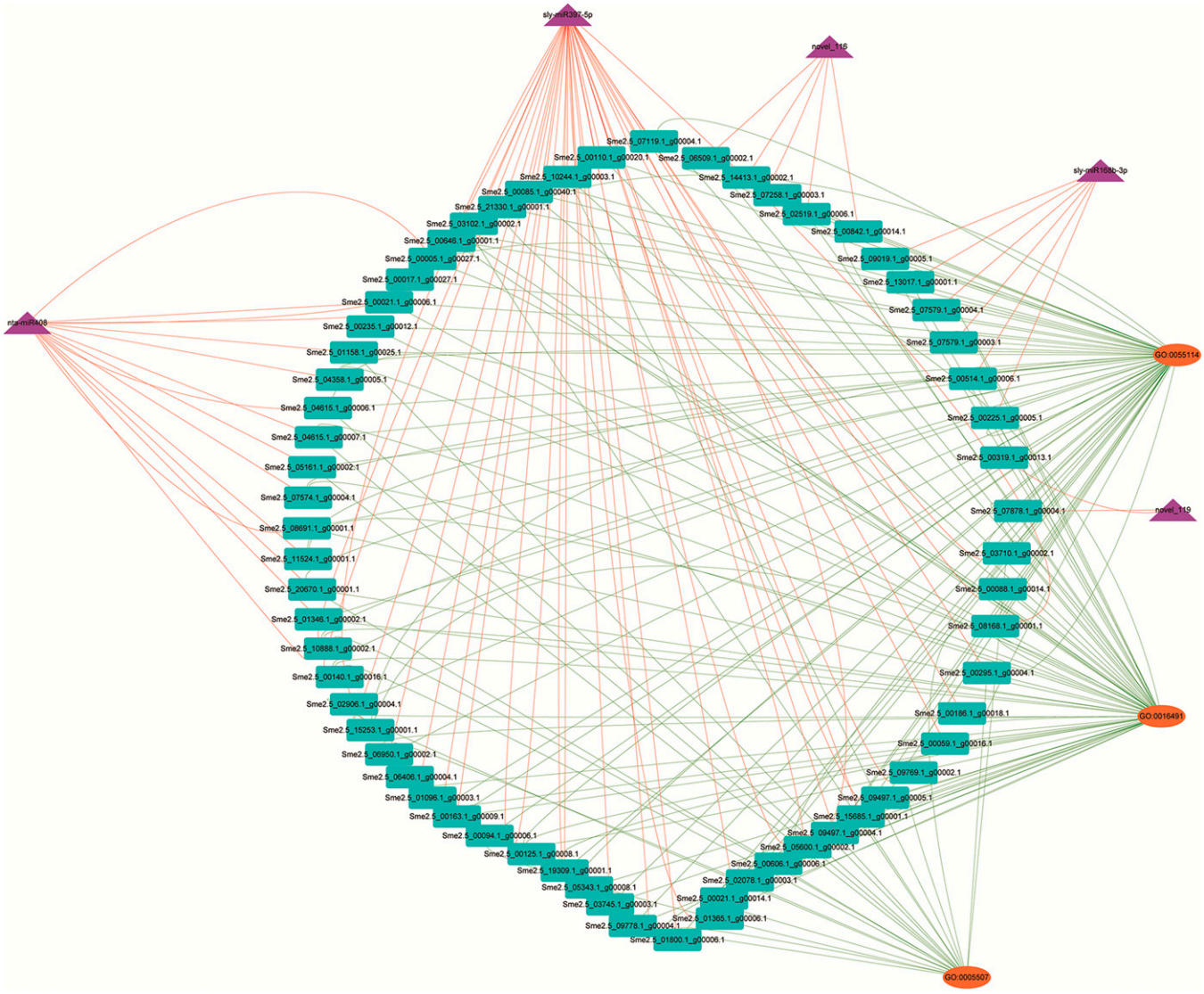

Fig. 5. Regulatory networks comprising Gene Ontology terms, differentially expressed microRNAs (DEMs), and their target genes in the sterile line 05ms and fertile line S63 of eggplant. Ellipses, triangles, and rectangles represent GO terms, DEMs, and target genes, respectively.

Downloaded from https://prime-pdf-watermark.prime-prod.pubfactory.com/ at 2025-07-30 via Open Access. This is an open access article distributed under the CC BY-NC-ND license (https://creativecommons.org/licenses/by-nc-nd/4.0/). https://creativecommons.org/licenses/by-nc-nd/4.0/

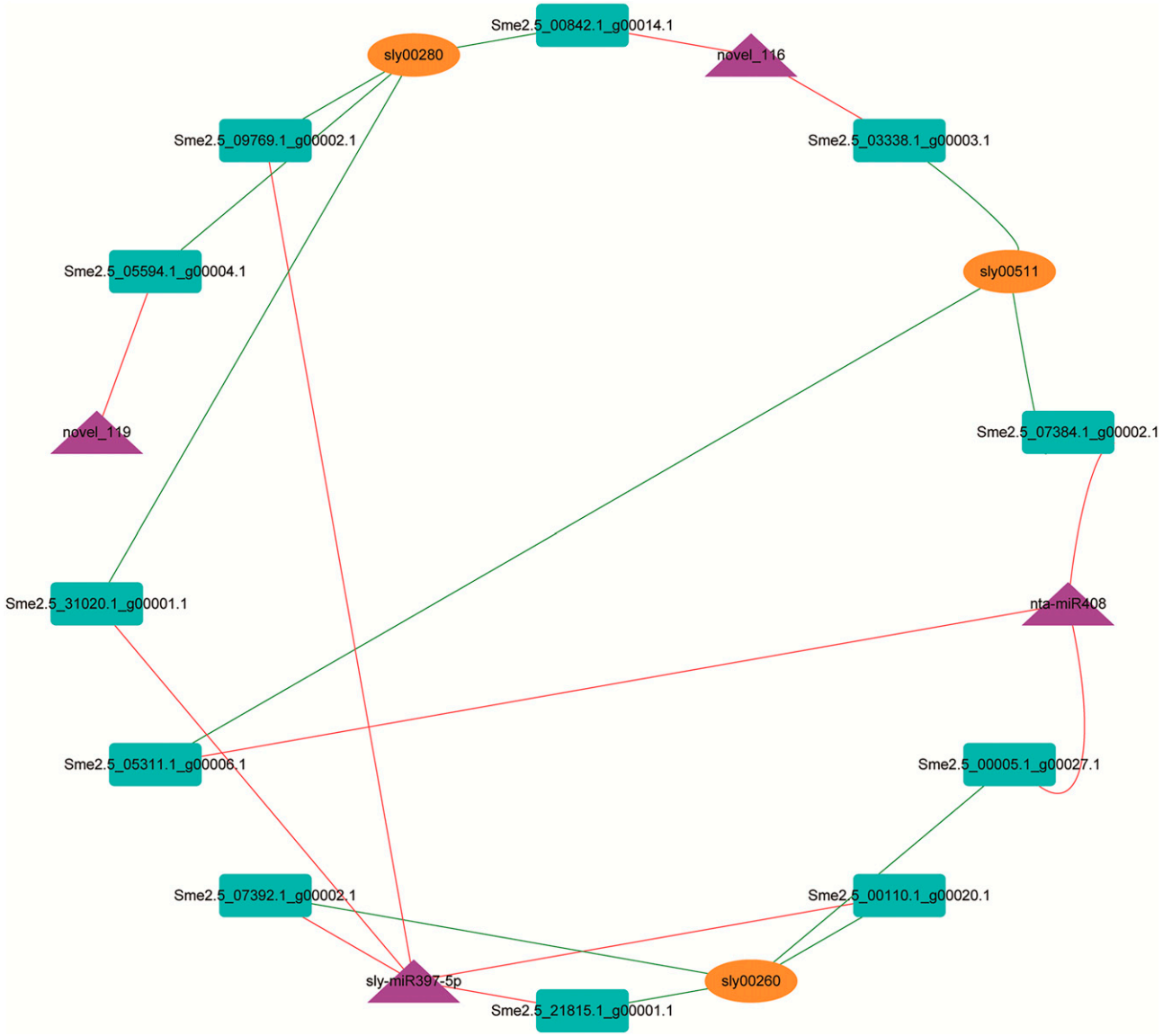

Fig. 6. Regulatory network comprising Kyoto Encyclopedia of Genes and Genomes pathways, differentially expressed microRNAs (DEMs), and their target genes in the sterile line 05ms and fertile line S63 of eggplant. Ellipses, triangles, and rectangles represent KEGG pathways, DEMs, and their target genes, respectively.

because they eliminate the need for an emasculation procedure, thereby reducing the cost of hybrid seed production. With rapidly developing sequencing technology, many plant genomes have been sequenced, and the resulting omics data are excellent resources for molecular studies (Song et al., 2019). miRNAs are important in regulation of plant anther development (Dong et al., 2020).

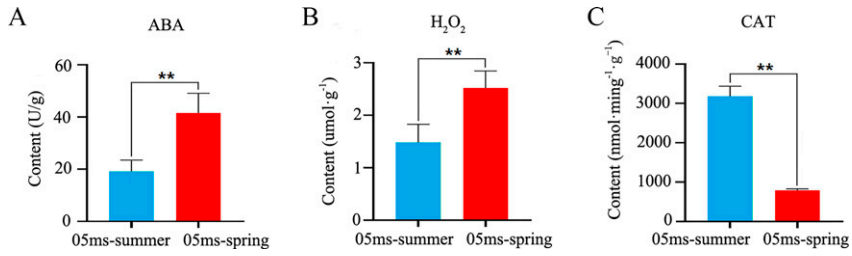

Fig. 7. The contents comparison of abscisic acid (ABA), hydrogen peroxide (H_2O_2), and catalase (CAT) between 05ms-spring and 05ms-summer in the sterile line 05ms. (**A**) ABA contents in 05ms-spring and 05ms-summer. (**B**) H_2O_2 contents in 05ms-spring and 05ms-summer. (**C**) CAT contents in 05ms-spring and 05ms-summer (05ms-spring = spring sterile period at low temperature in 05ms; 05ms-summer = summer fertile period at high temperature in 05ms). Error bars indicate the standard error of three biological replicates. Statistical significance was analyzed by a *t* test to compare 05ms-summer to 05ms-spring for each category in all statistical. **Significant at $P < 0.01$.

Downloaded from https://prime-pdf-watermark.prime-prod.pubfactory.com/ at 2025-07-30 via Open Access. This is an open access article distributed under the CC BY-NC-ND license (https://creativecommons.org/licenses/by-nc-nd/4.0/). https://creativecommons.org/licenses/by-nc-nd/4.0/

In this study, to determine the functions of miRNAs during eggplant rTGMS, miRNAs expression levels in the meiosis stage anthers from the rTGMS line 05ms and the homologous fertile line S63 were analyzed by high-throughput sequencing. This is the first report of a comprehensive comparison of miRNA expression levels between TGMS and temperature-insensitive eggplant lines.

ROS and male sterility. ROS homeostasis is critical for anther development, and H_2O_2 is a key factor in ROS production (Hameed et al., 2012). Antioxidant enzyme-mediated redox homeostasis was a key index to estimate the deleterious effects of ROS in anthers. Superoxide dismutase content decreases and H_2O_2 content increases in stamens during anther development of genic male sterile mutant in cotton (*Gossypium* sp.; Zheng et al., 2021). Enhanced CAT activities in rice anther help to eliminate oxidative damage through scavenging of ROS (Zhao et al., 2018b). Further, a rise in temperature during anthesis can stimulate significantly increased ROS content and malondialdehyde accumulation in anthers, thereby triggering pollen mortality in wheat (Dwivedi et al., 2019). In this study, GO analysis indicated that target genes were primarily enriched in redox-related terms. Elevated ABA levels can also cause ROS release (Yu et al., 2019) and our data show that ABA and H_2O_2 were higher and CAT levels markedly lower in the 05ms-spring than in 05ms-summer groups (Fig. 6); therefore, we propose that low temperature stress can induce ROS burst, which may result in anther abortion in rTGMS line of eggplant.

miR397-5P and male sterility. Many studies have demonstrated that miRNAs regulate gene expression by controlling transcription factors, which may be an important feature of miRNA function (Liu et al., 2016). Some transcription factors were identified as miRNA target genes in the tomato photoperiod-sensitive male sterility mutant *7B-1*, suggesting that they are associated with, or involved in, the regulation of male sterility (Omidvar et al., 2015). In this study, the expression level of miR397-5p in 05ms-spring was 29.45, whereas that in 05ms-summer was more than 6 times higher at 185.36. We speculate that low temperature severely inhibits miR397-5p expression. Target gene is key to understanding miRNA function. The four target gene ID numbers were presented by comparing the reference genome in 2019 and 2014 (Supplemental Table 8). *dyt1* is a bHLH transcription factor, plays a critical role in regulating tapetum development, and its alteration can directly lead to anther abortion (Cui et al., 2016). *dyt1* regulates a series of downstream genes, which are necessary for anther development, including *tapetal development and function 1*, *Aborted microspores*, and *Male sterility 1*, and interacts with many transcription factors (Gu et al., 2014). WRKY family genes respond to low temperature stress and affect plant stress resistance by participating in ABA signal transduction (Zhao et al., 2019). *LAC* genes encode key lignin biosynthesis enzymes (Xue et al., 2018). Lignin is a vital constituent part of the plant secondary cell wall and can improve mechanical support (Zhou et al., 2009). *LAC* was induced by ABA to positively regulated lignin synthesis and influence cell wall ductility (Li et al., 2020). Plant tissues with high *LAC* gene expression also have high levels of lignification (Wang et al., 2020). miR397 negatively regulated lignin content by slicing *LAC* transcription, thereby promoted plant defense (Wei et al., 2021). Thus, ABA participated in anther response to low temperature and formation of anther cell wall. Hence, miR397-5p likely regulates anther development and low temperature tolerance by negatively regulating these target gene expression in rTGMS line of eggplant.

Conclusions

The occurrence of male sterility in rTGMS line '05ms' involved many biological processes and metabolic pathways. This is the first report of miRNAs in the anthers of the male sterility in eggplant using high-throughput sequencing technology. According to the analysis results of sRNA-seq, qRT-PCR, and related physiological indexes, we identified 143 known miRNAs and 104 novel miRNAs, and found that three known miRNAs (miR168b, miR397, and miR408) and three novel miRNAs (Novel_116, Novel_119, and Novel_97) probably played an important role during anther development in '05ms'. Target prediction and annotation showed that these target genes enriched in plant hormone signal transduction and oxidation-reduction process. The regulatory networks analysis found the miR397-5p was the most important miRNA. We speculate that the anther abortion under low temperature conditions might be caused by the hormone imbalance, the destruction of antioxidant system, and the accumulation of H_2O_2. Our results will facilitate understanding of the molecular mechanism underlying miRNA regulation of fertility conversion and two-line cross-breeding in eggplant.

Literature Cited

Abdel-Ghany, S.E. and M. Pilon. 2008. MicroRNA-mediated systemic down-regulation of copper protein expression in response to low copper availability in *Arabidopsis*. J. Biol. Chem. 283(23):15932–15945, https://doi.org/10.1074/jbc.M801406200.

Betti, F., M.J. Ladera-Carmona, D.A. Weits, G. Ferri, S. Iacopino, G. Novi, B. Svezia, A.B. Kunkowska, A. Santaniello, A. Piaggesi, E. Loreti, and P. Perata. 2021. Exogenous miRNAs induce post-transcriptional gene silencing in plants. Nat. Plants 7(10):1379–1388, https://doi.org/10.1038/S41477-021-01005-W.

Concetta, D.M., L. Vittoria, P. Annalisa, and D.G. Laura. 2015. Role of redox homeostasis in hermos-tolerance under a climate change scenario. Ann. Bot. (Lond.) 116(4):487–496, https://doi.org/10.1093/aob/mcv071.

Cui, J., C.J. You, E.G. Zhu, Q. Huang, H. Ma, and F. Chang. 2016. Feedback regulation of DYT1 by interactions with downstream bHLH factors promotes DYT1 nuclear localization and anther development. Plant Cell 28(5):1078–1093, https://doi.org/10.1105/tpc.15.00986.

Devireddy, A.R., S.I. Zandalinas, Y. Fichman, and R. Mittler. 2021. Integration of reactive oxygen species and hormone signaling during abiotic stress. Plant J. 105(1):459–476, https://doi.org/10.1111/TPJ.15360.

Dong, Y., Y. Wang, F.W. Jin, L.J. Xin, and M.Y. Xu. 2020. Differentially expressed miRNAs in anthers may contribute to the fertility of a novel *Brassica napus* genic male sterile line CN12A. J. Integr. Agric. 19(7):1731–1742, https://doi.org/10.1016/S2095-3119(19)62780-2.

Dwivedi, S.K., S. Basu, S. Kumar, S. Kumari, and G. Kumar. 2019. Enhanced antioxidant enzyme activities in developing anther contributes to heat stress alleviation and sustains grain yield in wheat. Funct. Plant Biol. 46(12):1090, https://doi.org/10.1071/FP19016.

Feng, L., R. Xia, and Y.L. Liu. 2019. Comprehensive characterization of mirna and phas loci in the diploid strawberry (*Fragaria vesca*) genome. Hortic. Plant J. 5(6):255–267, https://doi.org/10.1016/j.hpj.2019.11.004.

Friedlander, M.R., S.D. Mackowiak, N. Li, W. Chen, and N. Rajewsky. 2011. miRDeep2 accurately identifies known and hundreds of novel microRNA genes in seven animal clades. Nucleic Acids Res. 40(1): 37–52, https://doi.org/10.1093/nar/gkr688.

Gu, J.N., J. Zhu, Y. Yu, X.D. Teng, Y. Lou, X.F. Xu, J.L. Liu, and Z.N. Yang. 2014. DYT1 directly regulates the expression of TDF1

Downloaded from https://prime-pdf-watermark.prime-prod.pubfactory.com/ at 2025-07-30 via Open Access. This is an open access article distributed under the CC BY-NC-ND license (https://creativecommons.org/licenses/by-nc-nd/4.0/). https://creativecommons.org/licenses/by-nc-nd/4.0/

for tapetum development and pollen wall formation in *Arabidopsis*. Plant J. 80(6):1005–1013, https://doi.org/10.1111/tpj.12694.
Guo, C.K., Y.Q. Jiang, M. Shi, X. Wu, and G. Wu. 2021. ABI5 acts downstream of miR159 to delay vegetative phase change in *Arabidopsis*. New Phytol. 231(1):339–350, https://doi.org/10.1111/NPH.17371.
Hameed, A., M. Goher, and N. Iqbal. 2012. Heat stress-induced cell death, changes in antioxidants, lipid peroxidation and protease activity in wheat leaves. J. Plant Growth Regul. 31(3):283–291, https://doi.org/10.1007/s00344-011-9238-4.
Hirakawa, H., K. Shirasawa, K. Miyatake, T. Nunome, S. Negoro, A. Ohyama, H. Yamaguchi, S. Sato, S. Isobe, S. Tabata, and H. Fukuoka. 2014. Draft genome sequence of eggplant (*Solanum melongena* L.): The representative solanum species indigenous to the old world. DNA Res. 21(6):649–660, https://doi.org/10.1093/dnares/dsu027.
Huang, M.D., Y.I. Caroline, and A.H.C. Huang. 2011. Transcriptomes of the anther sporophyte: Availability and uses. Plant Cell Physiol. 52(9):1459–1466, https://doi.org/10.1093/pcp/pcr088.
Jiang, J.X., P.F. Xu, Y.J. Li, Y.L. Li, X.R. Zhou, M.Y. Jiang, J.Y. Zhang, J.F. Zhu, W.R. Wang, and L.Y. Yang. 2021. Identification of miRNAs and their target genes in genic male sterility lines in *Brassica napus* by small RNA sequencing. BMC Plant Biol. 21(1):520, https://doi.org/10.1186/S12870-021-03306-W.
Kanehisa, M., Araki, M., Goto, S., Hattori, M., and Hirakawa, M. 2008. KEGG for linking genomes to life and the environment. Nucleic Acids Res. 36(Database):D480–D484, https://doi.org/10.1093/nar/gkm882.
Kozomara, A., M. Birgaoanu, and S. Griffiths-Jones. 2019. miRBase: From microRNA sequences to function. Nucleic Acids Res. 47(D1):D155–D162, https://doi.org/10.1093/nar/gky1141.
Langmead, B., C. Trapnell, M. Pop, and S.L. Salzberg. 2009. Ultrafast and memory-efficient alignment of short DNA sequences to the human genome. Genome Biol. 10(3):R25, https://doi.org/10.1186/gb-2009-10-3-r25.
Llave, C., Z.X. Xie, K.D. Kasschau, and J.C. Carrington. 2002. Cleavage of scarecrow-like mRNA targets directed by a class of *Arabidopsis* miRNA. Science 297(5589):2053–2056, https://doi.org/10.1126/science.1076311.
Li, B., X.P. Chen, Y.R. Wu, A.X. Gu, J.J. Zhang, S.X. Luo, X.R. Gao, J.J. Zhao, X.Q. Pan, and S.X. Shen. 2019. Gene characterization and molecular pathway analysis of reverse thermosensitive genic male sterility in eggplant (*Solanum melongena* L.). Hortic. Res.-England 6(1):118, https://doi.org/10.1038/s41438-019-0201-z.
Li, L.C., K.B. Yang, S.N. Wang, Y.F. Lou, C.L. Zhu, and Z.M. Gao. 2020. Genome-wide analysis of laccase genes in moso bamboo highlights PeLAC10 involved in lignin biosynthesis and in response to abiotic stresses. Plant Cell Rep. 39(6):751–763, https://doi.org/10.1007/s00299-020-02528-w.
Lin, Y., L. Zhang, Y. Zhao, Z. Wan, H. Liu, L. Zhang, and S. Zhou. 2020. Comparative analysis and functional identification of temperature-sensitive miRNA in *Arabidopsis* anthers. Biochem. Biophys. Res. Commun. 532(1):1–10, https://doi.org/10.1016/j.bbrc.2020.05.033.
Liu, Y.M., L. Zhang, T. Qiu, Z.F. Zhao, and M.J. Cao. 2016. Research progress on mechanisms of male sterility in plants based on high-throughput RNA sequencing. Hereditas 38(8):677–687, https://doi.org/10.16288/j.yczz.16-031.
Love, M.I., W. Huber, and S. Anders. 2014. Moderated estimation of fold change and dispersion for RNA-seq data with DESeq2. Genome Biol. 15(12):550, https://doi.org/10.1186/s13059-014-0550-8.
Mao, X., T. Cai, J.G. Olyarchuk, and L. Wei. 2005. Automated genome annotation and pathway identification using the KEGG orthology (KO) as a controlled vocabulary. Bioinformatics 21(19):3787–3793, https://doi.org/10.1093/bioinformatics/bti430.
Nawrocki, E.P., S.W. Burge, A. Bateman, J. Daub, R.Y. Eberhardt, S.R. Eddy, E.W. Floden, P.P. Gardner, T.A. Jones, J. Tate, and R.D. Finn. 2015. Rfam 12.0: Updates to the RNA families database. Nucleic Acids Res. 43(D1):D130–D137, https://doi.org/10.1093/nar/gku1063.
Omidvar, V., I. Mohorianu, T. Dalmay, and M. Fellner. 2015. Identification of miRNAs with potential roles in regulation of anther development and male-sterility in 7B-1 male-sterile tomato mutant. BMC Genomics 16(1):878, https://doi.org/10.1186/s12864-015-2077-0.
Schmittgen, T.D. and K.J. Livak. 2008. Analyzing real-time PCR data by the comparative C(T) method. Nat. Protoc. 3(6):1101–1108, https://doi.org/10.1038/nprot.2008.73.
Sheoran, I.S., A.R. Ross, D.J. Olson, and V.K. Sawhney. 2009. Differential expression of proteins in the wild type and male-sterile mutant anthers of tomato (*Solanum lycopersicum*): A proteomic analysis. J. Proteomics 71(6):624–636, https://doi.org/10.1016/j.jprot.2008.10.006.
Shi, Q.Q., X.X. Zhang, X. Li, L.J. Zhai, X.N. Luo, J.R. Luo, L.X. He, Y.L. Zhang, and L. Li. 2019. Identification of micrornas and their targets involved in paeonia rockii petal variegation using high-throughput sequencing. J. Amer. Soc. Hort. Sci. 144(2):118–129, https://doi.org/10.21273/JASHS04395-18.
Song, X., Y. Li, X. Cao, and Y. Qi. 2019. MicroRNAs and their regulatory roles in plant-environment interactions. Annu. Rev. Plant Biol. 70(1):489–525, https://doi.org/10.1146/annurev-arplant-050718-100334.
Sun, Y.J., X.G. Xiong, Q. Wang, L. Zhu, L. Wang, Y. He, and H.L. Zeng. 2021. Integrated analysis of small RNA, transcriptome, and degradome sequencing reveals the MiR156, MiR5488 and MiR399 are involved in the regulation of male sterility in PTGMS rice. Int. J. Mol. Sci. 22(5):2260, https://doi.org/10.3390/IJMS22052260.
Tang, Z.H., L.P. Zhang, C.G. Xu, S.H. Yuan, F.T. Zhang, Y.L. Zheng, and C.P. Zhao. 2012. Uncovering small RNA-mediated responses to cold stress in a wheat thermosensitive genic male-sterile line by deep sequencing. Plant Physiol. 159(2):721–738, https://doi.org/10.1104/pp.112.196048.
Tian, C.J., Z.L. Zuo, and J.L. Qiu. 2015. Identification and characterization of ABA-responsive microRNAs in rice. J. Genet. Genomics 42(7):393–402, https://doi.org/10.1016/j.jgg.2015.04.008.
Toppino, L., M. Kooiker, M. Lindner, L. Dreni, G.L. Rotino, and M.M. Kater. 2011. Reversible male sterility in eggplant (*Solanum melongena* L.) by artificial microRNA-mediated silencing of general transcription factor genes. Plant Biotechnol. J. 9(6):684–692, https://doi.org/10.1111/j.1467-7652.2010.00567.x.
Voinnet, O. 2009. Origin, biogenesis, and activity of plant microRNAs. Cell 136(4):669–687, https://doi.org/10.1016/j.cell.2009.01.046.
Wang, X., C.L. Zhuo, X.R. Xiao, X.Q. Wang, M. Docampo-Palacios, F. Chen, and R.A. Dixon. 2020. Substrate specificity of LACCASE8 facilitates polymerization of caffeyl alcohol for C-Lignin biosynthesis in the seed coat of *Cleome hassleriana*. Plant Cell 32(12):3825–3845, https://doi.org/10.1105/tpc.20.00598.
Wei, T., Tang, Y., Jia, P., Zeng, Y., Wang, B., Wu, P., Quan, Y., Chen, A., Li, Y., and Wu, J. 2021. A cotton lignin biosynthesis gene, GhLAC4, fine-tuned by ghr-miR397 modulates plant resistance against verticillium dahliae. Front Plant Sci. 12:743–795, https://doi.org/10.3389/fpls.2021.743795.
Wingett, S.W. and S. Andrews. 2018. FastQ Screen: A tool for multi-genome mapping and quality control. F1000Res. 7:1338, https://doi.org/10.12688/f1000research.15931.2.
Wu, H.J., Y.K. Ma, T. Chen, M. Wang, and X.J. Wang. 2012. PsRobot: A web-based plant small RNA meta-analysis toolbox. Nucleic Acids Res. 40(W1):W22–W28, https://doi.org/10.1093/nar/gks554.
Xue, C., J.L. Yao, M.F. Qin, M.Y. Zhang, A.C. Allan, D.F. Wang, and J. Wu. 2018. PbrmiR397a regulates lignification during stone cell development in pear fruit. Plant Biotechnol. J. 17(1):103–117, https://doi.org/10.1111/pbi.12950.
Young, M.D., M.J. Wakefield, G.K. Smyth, and A. Oshlack. 2010. goseq: Gene Ontology testing for RNA-seq: Accounting for selection bias. Genome Biol. 11(2):R14–R14, https://doi.org/10.1186/gb-2010-11-2-r14.
Yang, X., F. Liu, Y. Zhang, L. Wang, and Y.F. Cheng. 2017. Cold-responsive miRNAs and their target genes in the wild eggplant species

Downloaded from https://prime-pdf-watermark.prime-prod.pubfactory.com/ at 2025-07-30 via Open Access. This is an open access article distributed under the CC BY-NC-ND license (https://creativecommons.org/licenses/by-nc-nd/4.0/). https://creativecommons.org/licenses/by-nc-nd/4.0/

Solanum aculeatissimum. BMC Genomics 8(1):1000, https://doi.org/10.1186/s12864-017-4341-y.

Yoshida, T., Y. Fujita, K. Maruyama, J. Mogami, D. Todaka, K. Shinozaki, and K. Yamaguchi-Shinozaki. 2015. Four *Arabidopsis* AREB/ABF transcription factors function predominantly in gene expression downstream of SnRK2 kinases in abscisic acid signalling in response to osmotic stress. Plant Cell Environ. 38(1):35–49, https://doi.org/10.1111/pce.12351.

Yu, Y.W., J. Wang, S.H. Li, X. Kakan, Y. Zho, Y.C. Miao, F.F. Wang, H. Qin, and R.F. Huang. 2019. Ascorbic acid integrates the antagonistic modulation of ethylene and abscisic acid in the accumulation of reactive oxygen species. Plant Physiol. 179(4):1861–1875, https://doi.org/10.1104/pp.18.01250.

Zhang, Z.B., M.H. Hu, W.W. Xu, Y. Wang, K. Huang, C. Zhang, and J. Wen. 2021. Understanding the molecular mechanism of anther development under abiotic stresses. Plant Mol. Biol. 105(1-2):1–10, https://doi.org/10.1007/s11103-020-01074-z.

Zhao, Q., L.J. Zhou, J.C. Liu, Z.Z. Cao, X.X. Du, F.D. Huang, G. Pan, and F.M. Cheng. 2018b. Involvement of CAT in the detoxification of HT-induced ROS burst in rice anther and its relation to pollen fertility. Plant Cell Rep. 37(5):741–757, https://doi.org/10.1007/s00299-018-2264-y.

Zhao, X.Y., C.H. Qi, H. Jiang, C.X. You, Q.M. Guan, F.W. Ma, Y.Y. Li, and Y.J. Hao. 2019. The MdWRKY31 transcription factor binds to the MdRAV1 promoter to mediate ABA sensitivity. Hortic. Res.-England 6(1):66, https://doi.org/10.1038/s41438-019-0147-1.

Zheng, H.L., R.J. Wang, Q.M. Jiang, D.D. Zhang, R.R. Mu, Y.H. Xu, V.E. Nnaemeka, J. Mei, Y.Y. Zhao, F.F. Cai, D.L. Yu, Y.Q. Sun, and L.P. Ke. 2021. Identification and functional analysis of a pollen fertility-associated gene GhGLP4 of *Gossypium hirsutum* L. Theor. Appl. Genet. 134(1):3237–3247, https://doi.org/10.1007/S00122-021-03888-X.

Zheng, L.J., P. Nagpal, G. Villarino, B. Trinidad, L. Bird, Y. Huang, and J.W. Reed. 2019. miR167 limits anther growth to potentiate anther dehiscence. Development 146(14):14, https://doi.org/10.1242/dev.174375.

Zhou, L., J.H. Chen, Z.Z. Li, X.X. Li, X.D. Hu, Y. Huang, X.K. Zhao, C.Z. Liang, Y. Wang, L. Sun, M. Shi, X.H. Xu, F. Shen, M.S. Chen, Z.J. Han, Z.Y. Peng, Q.N. Zhai, J. Chen, Z.F. Zhang, R.L. Yang, J.X. Ye, Z.C. Guan, H.M. Yang, Y.T. Gui, J. Wang, Z.M. Cai, and X.Q. Zhang. 2010. Integrated profiling of microRNAs and mRNAs: MicroRNAs located on Xq27.3 associate with clear cell renal cell carcinoma. PLoS One 5(12):e15224, https://doi.org/10.1371/journal.pone.0015224.

Zhou, H., M. He, J. Li, L. Chen, Z.F. Huang, S.Y. Zheng, L.Y. Zhu, E. Ni, D.G. Jiang, B.R. Zhao, and C.X. Zhuang. 2016. Development of commercial thermo-sensitive genic male sterile rice accelerates hybrid rice breeding using the CRISPR/Cas9-mediated TMS5 editing system. Sci Rep-UK 6(1):37395, https://doi.org/10.1038/srep37395.

Zhou, J.L., C. Lee, R.Q. Zhong, and Z.H. Ye. 2009. MYB58 and MYB63 are transcriptional activators of the lignin biosynthetic pathway during secondary cell wall formation in *Arabidopsis*. Plant Cell 21(1):248–266, https://doi.org/10.1105/tpc.108.063321.

Downloaded from https://prime-pdf-watermark.prime-prod.pubfactory.com/ at 2025-07-30 via Open Access. This is an open access article distributed under the CC BY-NC-ND license (https://creativecommons.org/licenses/by-nc-nd/4.0/). https://creativecommons.org/licenses/by-nc-nd/4.0/

Supplemental Fig. 1. Morphological comparison of flowers in the sterile line 05ms and fertile line S63 of eggplant. (**A**) The phenotype of flower in 05ms. (**B**) The phenotype of flower in S63.

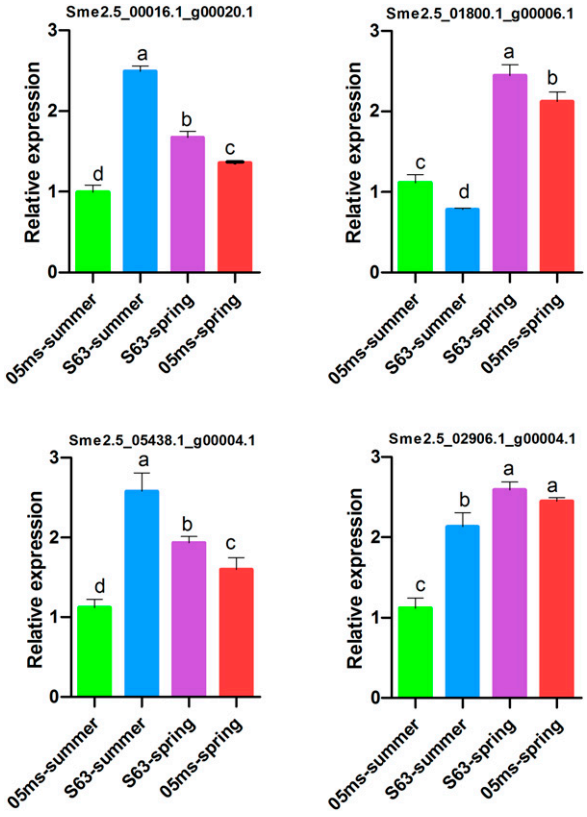

Supplemental Fig. 2. Quantitative real-time polymerase chain reaction confirmation of target genes at different periods in the sterile line 05ms and fertile line S63 of eggplant: 05ms-spring = spring sterile period at low temperature in 05ms; 05ms-summer = summer fertile period at high temperature in 05ms; S63-spring = spring fertile period at low temperature in S63; S63-summer = summer fertile period at high temperature in S63. *Sme2.5_00016.1_g00020.1*, *Sme2.5_01800.1_g00006.1*, *Sme2.5_05438.1_g00004.1*, and *Sme2.5_02906.1_g00004.1* are the four target genes. Different letters above the bars represent significant differences at $P < 0.05$ according to Duncan's multiple range test.

Downloaded from https://prime-pdf-watermark.prime-prod.pubfactory.com/ at 2025-07-30 via Open Access. This is an open access article distributed under the CC BY-NC-ND license (https://creativecommons.org/licenses/by-nc-nd/4.0/). https://creativecommons.org/licenses/by-nc-nd/4.0/

Supplemental Table 1. The primers information of quantitative real time polymerase chain reaction validation of microRNAs and their target genes in eggplant.

Target gene	Forward (5′ to 3′)	Reverse (5′ to 3′)
Sme2.5_00016.1_g00020.1	TGTTCGCAAGCACATTGAGC	TTTTTGGGTACGGGCATGTC
Sme2.5_00110.1_g00016.1	TATTGGGCTTGACGATGCTG	AGCCTTCCTTGCAAGAACAC
Sme2.5_00166.1_g00017.1	ATGGGCTGCAATTGCTTCAC	AGCACTGTTCATGAGTCTGAGG
Sme2.5_01236.1_g00003.1	AACTAAAGGCCGCAATTCGC	CCTTGCAGCTTGTTTTGTGC
Sme2.5_01800.1_g00006.1	TCGTTGCTTTTCACGGTTGG	ATGCCGAAGAAATGCGCTTG
Sme2.5_01957.1_g00005.1	TGCAACCTGTTTCTGCATCC	AGGCAGATGCTTTTGGTGTC
Sme2.5_03745.1_g00003.1	AAACGCCACAAGAACACTGC	TCTCTTTCTCAGACAGCATCCG
Sme2.5_05438.1_g00004.1	TTCAAGTGGCTCACATTGGC	TTTAGAGGCAGTCACACTGGTG
Sme2.5_02906.1_g00004.1	TTAACCCTTGCCCAACATGC	TTGCTGGAAAATCCGTCGTG
Sme2.5_01553.1_g00004.1	AAACCAACGTACTGCAAGCG	AAACACTTGTGGGACAGTGC
Actin[i]	TTACTCATTCACCACCACAG	ACCATCGGGAAGCTCATAG
novel_97	GCGCAACGTGTTGGATATTGATATTCTT	—
novel_116	GCGTTTTGACTGCCTCTAATACAAG	—
novel_119	GCGCAGTGCTCTTTGAATTTAGATAAAT	—
sly-miR168b-3p	CCCGCCTTGCATCAACTGAAT	—
sly-miR397–5P	ATTGAGTGCAGCGTTGATGA	—
nta-miR408	TGCACTGCCTCTTCCCTGGCT	—
U6[ii]	TCTAACAGTGTAGTTTGTCCCTTCG	—

[i] Actin was the reference gene for mRNA.
[ii] U6 was the reference gene for microRNA.

Supplemental Table 2. Quality statistics for small RNA sequencing data at different periods in the sterile line 05ms and fertile line S63 of eggplant.

							Clean reads	
Sample[i]	Raw reads, n	Bases (G)	Error rate, %	Q20, %[ii]	Q30, %[iii]	GC content, %	n	%
S63-summer1	15,431,011	0.772	0.0001	0.9935	0.9742	0.5001	14,859,280	96.29%
S63-summer2	11,725,861	0.586	0.0001	0.9925	0.9712	0.513	11,265,962	96.08%
S63-summer3	13,799,582	0.690	0.0001	0.9932	0.9728	0.4891	13,390,190	97.03%
S63-spring1	14,926,424	0.746	0.0001	0.9936	0.9749	0.4908	14,738,573	98.74%
S63-spring2	13,406,802	0.670	0.0001	0.987	0.9598	0.4999	13,083,603	97.59%
S63-spring3	13,312,690	0.666	0.0001	0.9935	0.9741	0.4954	12,952,273	97.29%
05ms-summer1	13,657,109	0.683	0.0001	0.9944	0.9772	0.4657	13,476,123	98.67%
05ms-summer2	13,630,980	0.682	0.0001	0.9946	0.9768	0.4618	13,460,662	98.75%
05ms-summer3	15,190,866	0.760	0.0001	0.9945	0.977	0.4689	14,984,438	98.64%
05ms-spring1	13,970,705	0.699	0.0001	0.9916	0.9697	0.4936	13,447,354	96.25%
05ms-spring2	13,582,149	0.679	0.0001	0.9905	0.9676	0.4613	13,010,691	95.79%
05ms-spring3	13,639,248	0.682G	0.0001	0.9928	0.9728	0.4595	13,144,240	96.37%

[i] S63-summer = summer fertile period at high temperature in S63 (S63-summer1, S63-summer2, and S63-summer3 were the three biological repeats); S63-spring = spring fertile period at low temperature in S63 (S63-spring1, S63-spring2, and S63-spring3 were the three biological repeats); 05ms-summer = summer fertile period at high temperature in 05ms (05ms-summer1, 05ms-summer2, and 05ms-summer3 were the three biological repeats); 05ms-spring = spring sterile period at low temperature in 05ms (05ms-spring1, 05ms-spring2, and 05ms-spring3 were the three biological repeats).
[ii] Q20 = percentage of bases with Phred value more than 20 in the total bases.
[iii] Q30 = percentage of bases with Phred value more than 30 in the total bases.

Downloaded from https://prime-pdf-watermark.prime-prod.pubfactory.com/ at 2025-07-30 via Open Access. This is an open access article distributed under the CC BY-NC-ND license (https://creativecommons.org/licenses/by-nc-nd/4.0/). https://creativecommons.org/licenses/by-nc-nd/4.0/

Supplemental Table 3. Mapping statistics to the reference genomes in 12 small RNA (sRNA) libraries derived from the sterile line 05ms and fertile line S63 of eggplant.

	sRNA			+ Mapped sRNA		– Mapped sRNA	
Sample[i]	Total reads, n	Mapped reads, n	%	Mapped reads, n	%	Mapped reads, n	%
S63-summer1	8,279,842	7,778,339	93.94	4,941,506	59.68	2,836,833	34.26
S63-summer2	5,373,114	5,085,627	94.65	3,345,816	62.27	1,739,811	32.38
S63-summer3	9,043,949	8,487,832	93.85	5,338,099	59.02	3,149,733	34.83
S63-spring1	12,665,324	11,937,446	94.25	8,050,251	63.56	3,887,195	30.69
S63-spring2	10,348,911	9,735,434	94.07	6,496,229	62.77	3,239,205	31.30
S63-spring3	10,276,720	9,704,737	94.43	6,549,154	63.73	3,155,583	30.71
05ms-summer1	11,903,426	11,154,058	93.70	6,890,987	57.89	4,263,071	35.81
05ms-summer2	12,161,809	11,380,868	93.58	7,006,263	57.61	4,374,605	35.97
05ms-summer3	12,747,309	11,954,558	93.78	7,427,333	58.27	4,527,225	35.52
05ms-spring1	7,925,178	7,442,319	93.91	4,755,057	60.00	2,687,262	33.91
05ms-spring2	11,632,421	10,820,742	93.02	6,669,084	57.33	4,151,658	35.69
05ms-spring3	12,038,859	11,229,873	93.28	6,901,272	57.32	4,328,601	35.96

[i] S63-summer = summer fertile period at high temperature in S63 (S63-summer1, S63-summer2, and S63-summer3 were the three biological repeats); S63-spring = spring fertile period at low temperature in S63 (S63-spring1, S63-spring2, and S63-spring3 were the three biological repeats); 05ms-summer = summer fertile period at high temperature in 05ms (05ms-summer1, 05ms-summer2, and 05ms-summer3 were the three biological repeats); 05ms-spring = spring sterile period at low temperature in 05ms (05ms-spring1, 05ms-spring2, and 05ms-spring3 were the three biological repeats).

Downloaded from https://prime-pdf-watermark.prime-prod.pubfactory.com/ at 2025-07-30 via Open Access. This is an open access article distributed under the CC BY-NC-ND license (https://creativecommons.org/licenses/by-nc-nd/4.0/). https://creativecommons.org/licenses/by-nc-nd/4.0/

Supplemental Table 4. Detailed information of the differentially expressed microRNAs (miRNAs) at different periods in the sterile line 05ms and fertile line S63 of eggplant.

	TPM[i]				05ms-spring vs. S63-spring			05ms-spring vs. 05ms-summer		
miRNA_ID	S63-summer	S63-spring	05ms-summer	05ms-spring	Log2FoldChange	Adjusted *P*	Significant	Log2FoldChange	Adjusted *P*	Significant
novel_97	685.49	295.93	718.76	3192.99	1.9483	2.38E-06	Up	1.6801	2.36E-06	Up
sly-miR397-5p	269.1	52.73	185.36	29.45	−1.9877	0.0058	Down	−2.1693	3.88E-05	Down
nta-miR408	1399.61	615.2	736.92	412.51	−1.9682	0	Down	−0.9945	0.0058	Down
novel_116	120.62	50.23	146.53	444.67	1.7088	0.003	Up	1.1343	0.0087	Up
novel_119	28.52	27.29	51.78	256.6	1.6406	0.0438	Up	1.4033	0.0204	Up
sly-miR168b-3p	1217.02	608.44	1084.41	906.06	−0.8966	0.0044	Down	−0.5019	0.0292	Down

[i] S63-summer = summer fertile period at high temperature in S63; S63-spring = spring fertile period at low temperature in S63; 05ms-summer = summer fertile period at high temperature in 05ms; 05ms-spring = spring sterile period at low temperature in 05ms.
TPM = transcripts per million.

Downloaded from https://prime-pdf-watermark.prime-prod.pubfactory.com/ at 2025-07-30 via Open Access. This is an open access article distributed under the CC BY-NC-ND license (https://creativecommons.org/licenses/by-nc-nd/4.0/). https://creativecommons.org/licenses/by-nc-nd/4.0/

Supplemental Table 5. The quantitative real time polymerase chain reaction (qRT-PCR) validation of differential expressed microRNAs (miRNAs) at different periods in the sterile line 05ms and fertile line S63 of eggplant.

		small RNA-seq			qRT-PCR		
miRNA	Material[1]	TPM	*SD*	*SE*	Relative expression	*SD*	*SE*
sly-miR168b-3p	05ms-summer	1084.41	167.19	96.53	1.00	0.00	0.00
	S63-summer	1217.02	654.26	377.75	7.51	1.66	0.96
	S63-spring	608.44	60.9	35.16	0.21	0.01	0.00
	05ms-spring	906.06	158.8	91.68	0.36	0.01	0.01
sly-miR397–5P	05ms-summer	185.36	59.61	34.42	1.00	0.00	0.00
	S63-summer	269.10	193.76	111.87	1.52	0.09	0.05
	S63-spring	52.73	30.08	17.36	0.48	0.05	0.03
	05ms-spring	29.45	14.79	8.54	0.39	0.03	0.02
nta-miR408	05ms-summer	736.92	90.44	52.22	1.00	0.00	0.00
	S63-summer	1399.61	890.45	514.12	7.89	1.48	0.85
	S63-spring	615.20	112.83	65.15	0.36	0.02	0.01
	05ms-spring	412.51	153.02	88.35	0.22	0.01	0.01
novel_97	05ms-summer	718.76	250.21	144.47	1.00	0.00	0.00
	S63-summer	685.49	163.34	94.31	3.35	0.17	0.1
	S63-spring	295.93	151.5	87.47	0.78	0.11	0.06
	05ms-spring	3192.99	1490.3	860.45	65.92	19.53	11.27
novel_116	05ms-summer	146.53	46.35	26.76	1.00	0.00	0.00
	S63-summer	120.62	36.87	21.29	0.30	0.03	0.02
	S63-spring	50.23	36.60	21.13	0.19	0.04	0.02
	05ms-spring	444.67	175.24	101.18	1.55	0.17	0.10
novel_119	05ms-summer	51.78	23.59	13.62	1.00	0.00	0.00
	S63-summer	28.52	14.36	8.29	0.10	0.01	0.01
	S63-spring	27.29	32.55	18.79	0.19	0.04	0.02
	05ms-spring	256.60	165.56	95.59	4.82	0.70	0.40

[1] 05ms-summer = summer fertile period at high temperature in 05ms; S63-summer = summer fertile period at high temperature in S63; S63-spring = spring fertile period at low temperature in S63; 05ms-spring = spring sterile period at low temperature in 05ms.
TPM = transcripts per million; *SD* = standard deviation; *SE* = standard error.

Supplemental Table 6. The first 20 enrichment Gene Ontology (GO) terms on target genes of the six differentially expressed microRNAs in the sterile line 05ms and fertile line S63 of eggplant.

GO accession	Description	Term type	*P* value	Adjusted *P*	DEG item
GO:0005507	Copper ion binding	molecular_function	2.93E-14	1.41E-10	21
GO:0055114	Oxidation-reduction process	biological_process	1.42E-05	0.026051	59
GO:0016491	Oxidoreductase activity	molecular_function	1.63E-05	0.026051	60
GO:0010374	Stomatal complex development	biological_process	0.00093505	0.49922	2
GO:0048580	Regulation of post-embryonic development	biological_process	0.00093505	0.49922	2
GO:0048582	Positive regulation of post-embryonic development	biological_process	0.00093505	0.49922	2
GO:0090558	Plant epidermis development	biological_process	0.00093505	0.49922	2
GO:2000038	Regulation of stomatal complex development	biological_process	0.00093505	0.49922	2
GO:2000123	Positive regulation of stomatal complex development	biological_process	0.00093505	0.49922	2
GO:0000724	Double-strand break repair via homologous recombination	biological_process	0.0012165	0.58452	2
GO:0008608	Attachment of spindle microtubules to kinetochore	biological_process	0.0032414	1	5
GO:0002115	Store-operated calcium entry	biological_process	0.0035942	1	3
GO:0010959	Regulation of metal ion transport	biological_process	0.0035942	1	3
GO:0043269	Regulation of ion transport	biological_process	0.0035942	1	3
GO:0051924	Regulation of calcium ion transport	biological_process	0.0035942	1	3
GO:2001256	Regulation of store-operated calcium entry	biological_process	0.0035942	1	3
GO:0034453	Microtubule anchoring	biological_process	0.0041243	1	5
GO:0015298	Solute:cation antiporter activity	molecular_function	0.0044125	1	4
GO:0015299	Solute:proton antiporter activity	molecular_function	0.0044125	1	4
GO:0019773	Proteasome core complex, alpha-subunit complex	cellular_component	0.0047891	1	3

DEG = differentially expressed gene.

Downloaded from https://prime-pdf-watermark.prime-prod.pubfactory.com/ at 2025-07-30 via Open Access. This is an open access article distributed under the CC BY-NC-ND license (https://creativecommons.org/licenses/by-nc-nd/4.0/). https://creativecommons.org/licenses/by-nc-nd/4.0/

Supplemental Table 7. The 72 enrichment Kyoto Encyclopedia of Genes and Genomes (KEGG) pathways on target genes of the six differentially expressed microRNAs in the sterile line 05ms and fertile line S63 of eggplant.

KEGG term	ID[i]	Input number	Background number	*P* value	Adjusted *P* value
Other glycan degradation	sly00511	3	13	0.002087408	0.150293372
Valine, leucine and isoleucine degradation	sly00280	4	57	0.017789953	0.640438321
Glycine, serine and threonine metabolism	sly00260	4	67	0.029223302	0.70135926
Zeatin biosynthesis	sly00908	3	50	0.056226214	0.781192236
Homologous recombination	sly03440	3	55	0.069858077	0.781192236
Lipoic acid metabolism	sly00785	1	5	0.094650857	0.781192236
Spliceosome	sly03040	6	185	0.095023049	0.781192236
Ether lipid metabolism	sly00565	2	30	0.096674881	0.781192236
Ubiquitin mediated proteolysis	sly04120	5	152	0.116644795	0.781192236
Other types of O-glycan biosynthesis	sly00514	1	7	0.124177323	0.781192236
SNARE interactions in vesicular transport	sly04130	2	44	0.174516072	0.781192236
Riboflavin metabolism	sly00740	1	11	0.180387728	0.781192236
Monoterpenoid biosynthesis	sly00902	1	11	0.180387728	0.781192236
Sulfur relay system	sly04122	1	12	0.193870399	0.781192236
Lysine biosynthesis	sly00300	1	13	0.207132484	0.781192236
Biosynthesis of amino acids	sly01230	6	236	0.208075978	0.781192236
Biosynthesis of secondary metabolites	sly01110	21	1036	0.209148395	0.781192236
Arachidonic acid metabolism	sly00590	1	14	0.220177572	0.781192236
Folate biosynthesis	sly00790	1	15	0.233009196	0.781192236
Plant hormone signal transduction	sly04075	7	301	0.243606088	0.781192236
2-oxocarboxylic acid metabolism	sly01210	2	62	0.283423371	0.781192236
Valine, leucine and isoleucine biosynthesis	sly00290	1	24	0.339442942	0.781192236
mRNA surveillance pathway	sly03015	3	124	0.347123517	0.781192236
Glycosylphosphatidylinositol (GPI)-anchor biosynthesis	sly00563	1	25	0.350321998	0.781192236
Carbon fixation in photosynthetic organisms	sly00710	2	80	0.391329807	0.781192236
Pantothenate and CoA biosynthesis	sly00770	1	29	0.392085027	0.781192236
Tryptophan metabolism	sly00380	1	30	0.402101651	0.781192236
Steroid biosynthesis	sly00100	1	31	0.411954127	0.781192236
Fatty acid elongation	sly00062	1	33	0.431177296	0.781192236
Diterpenoid biosynthesis	sly00904	1	33	0.431177296	0.781192236
Tropane, piperidine and pyridine alkaloid biosynthesis	sly00960	1	33	0.431177296	0.781192236
Propanoate metabolism	sly00640	1	33	0.431177296	0.781192236
Fatty acid metabolism	sly01212	2	90	0.448213282	0.781192236
Regulation of autophagy	sly04140	1	35	0.44977542	0.781192236
Nitrogen metabolism	sly00910	1	35	0.44977542	0.781192236
Photosynthesis	sly00195	2	91	0.453740377	0.781192236
Glycerophospholipid metabolism	sly00564	2	94	0.470130897	0.781192236
Phagosome	sly04145	2	94	0.470130897	0.781192236
Carotenoid biosynthesis	sly00906	1	38	0.476544687	0.781192236
Ubiquinone and other terpenoid-quinone biosynthesis	sly00130	1	38	0.476544687	0.781192236
Cysteine and methionine metabolism	sly00270	2	98	0.491524106	0.781192236
Basal transcription factors	sly03022	1	40	0.493667219	0.781192236
Biosynthesis of unsaturated fatty acids	sly01040	1	40	0.493667219	0.781192236
Pentose and glucuronate interconversions	sly00040	2	103	0.517493436	0.781192236
Glutathione metabolism	sly00480	2	108	0.542573475	0.781192236
Fatty acid degradation	sly00071	1	49	0.564079662	0.781192236
beta-Alanine metabolism	sly00410	1	49	0.564079662	0.781192236
alpha-Linolenic acid metabolism	sly00592	1	49	0.564079662	0.781192236
Proteasome	sly03050	1	50	0.571275429	0.781192236
RNA degradation	sly03018	2	114	0.571463388	0.781192236
DNA replication	sly03030	1	51	0.57835306	0.781192236
Alanine, aspartate and glutamate metabolism	sly00250	1	51	0.57835306	0.781192236
Metabolic pathways	sly01100	32	1961	0.588655869	0.781192236
Glycolysis/gluconeogenesis	sly00010	2	122	0.607902159	0.781192236
Terpenoid backbone biosynthesis	sly00900	1	56	0.612035608	0.781192236
Carbon metabolism	sly01200	4	253	0.613360259	0.781192236

(Continued on next page)

Downloaded from https://prime-pdf-watermark.prime-prod.pubfactory.com/ at 2025-07-30 via Open Access. This is an open access article distributed under the CC BY-NC-ND license (https://creativecommons.org/licenses/by-nc-nd/4.0/). https://creativecommons.org/licenses/by-nc-nd/4.0/

Supplemental Table 7. (Continued)

KEGG term	ID[i]	Input number	Background number	*P* value	Adjusted *P* value
Citrate cycle (TCA cycle)	sly00020	1	57	0.618443853	0.781192236
Glycerolipid metabolism	sly00561	1	63	0.654741809	0.812782935
Glyoxylate and dicarboxylate metabolism	sly00630	1	67	0.677011032	0.826182954
Phenylalanine metabolism	sly00360	2	152	0.723622983	0.864418711
Ribosome	sly03010	5	365	0.732354742	0.864418711
Aminoacyl-tRNA biosynthesis	sly00970	1	87	0.768662542	0.877466404
Ribosome biogenesis in eukaryotes	sly03008	1	90	0.779970137	0.877466404
Pyruvate metabolism	sly00620	1	90	0.779970137	0.877466404
Phenylpropanoid biosynthesis	sly00940	2	190	0.827751972	0.916894492
Starch and sucrose metabolism	sly00500	2	204	0.856257374	0.934098954
Amino sugar and nucleotide sugar metabolism	sly00520	1	123	0.873329514	0.938503358
Protein processing in endoplasmic reticulum	sly04141	2	238	0.908495808	0.948001054
Oxidative phosphorylation	sly00190	1	152	0.922137021	0.948001054
Purine metabolism	sly00230	1	154	0.924710472	0.948001054
RNA transport	sly03013	1	167	0.939494959	0.948001054
Plant-pathogen interaction	sly04626	1	176	0.948001054	0.948001054

[i] KEGG address.

Supplemental Table 8. The genetic information of four key target genes of the six differentially expressed microRNAs in reference genome between 2014 and 2019.

Gene_id[i] (2014)	Gene_id[i] (2019)	Chromesome	KEGG	GO	Swissport annotation
Sme2.5_00016.1_g00020.1	Smechr0700082	E07	K02888	GO:0003700 GO:0006355 GO:0043565	Probable WRKY transcription factor 32 OS=*Arabidopsis thaliana* OX=3702 GN=WRKY32 PE=2 SV=1
Sme2.5_01800.1_g00006.1	Smechr1002355	E10	K05909	GO:0005507 GO:0016491 GO:0055114	Laccase-4 OS=*A. thaliana* OX=3702 GN=IRX12 PE=2 SV=2
Sme2.5_05438.1_g00004.1	Smechr0201865	E02	K07198	GO:0046983	Transcription factor dyt1 OS=*A. thaliana* OX=3702 GN=dyt1 PE=2 SV=1
Sme2.5_02906.1_g00004.1	Smechr0900622	E09	K05909	GO:0005507 GO:0016491 GO:0055114	Laccase-4 OS=*A. thaliana* OX=3702 GN=IRX12 PE=2 SV=2

[i] Address of gene.
KEGG = Kyoto Encyclopedia of Genes and Genomes; GO = Gene Ontology.

Downloaded from https://prime-pdf-watermark.prime-prod.pubfactory.com/ at 2025-07-30 via Open Access. This is an open access article distributed under the CC BY-NC-ND license (https://creativecommons.org/licenses/by-nc-nd/4.0/). https://creativecommons.org/licenses/by-nc-nd/4.0/